

# Pull-out Strengths of GFRP-Concrete Bond Exposed to Applied Environmental Conditions

Muhammad Ikramul Kabir<sup>1)\*</sup>, Bijan Samali<sup>1)</sup>, and Rijun Shrestha<sup>2)</sup>

(Received December 6, 2015, Accepted September 28, 2016, Published online December 27, 2016)

**Abstract:** This paper presents results of an experimental investigation on the behaviour of bond between external glass fibre reinforced polymer reinforcement and concrete exposed to three different environmental conditions, namely, temperature cycles, wet–dry cycles and outdoor environment separately for extended durations. Single shear tests (pull-out test) were conducted to investigate bond strengths (pull-out strengths) of control (unexposed) and exposed specimens. Effect of the exposure conditions on the compressive strength of concrete were also investigated separately to understand the effect of changing concrete compressive strength on the pull-out strength. Based on the comparison of experimental results of exposed specimens to control specimens in terms of bond strengths, failure modes and strain profiles, the most significant degradation of pull-out strength was observed in specimens exposed to outdoor environment, whereas temperature cycles did not cause any deterioration of strength.

**Keywords:** GFRP-concrete bond, wet lay-up, pull-out strength, failure mode, strain profile, temperature cycles, wet–dry cycles, outdoor environment.

## 1. Introduction

Application of fibre reinforced polymer (FRP) composites in rehabilitation of concrete structures has recently been considered as a suitable technique due to advantageous properties of FRP such as high strength to weight ratio, high corrosion resistance and ease in application process. Extensive research has been conducted on FRP material for both its short and long term performance. In addition, many studies can be found in literature on the FRP-concrete bond system for short term loads due to the dependence of the performance of FRP bonded RC structures on the effective stress transfer between FRP and concrete. However, according to authors' knowledge, research studies on the long term effects of environmental conditions on FRP-concrete bond are still limited.

Among the available studies, some research focused on the durability of concrete beams strengthened with FRP and investigated the changes in ultimate beam strength and stiffness after various environmental exposures, whereas other research conducted similar investigation on the bond strength between FRP and concrete under aggressive

environment. Various environmental conditions such as freeze–thaw cycles, wet–dry cycles, combined environmental cycles, boiling water and UV radiation, hydrothermal ageing under constant temperature and humidity, and dry heat were applied by Chajes et al. (1995), Toutanji and Gómez (1997), Myers et al. (2001), Li et al. (2002) and Grace (2004) to investigate the long term performance of FRP strengthened concrete beams in terms of ultimate strength and/or stiffness of beams. Chajes et al. (1995) reported wet–dry cycles as slightly more severe than freeze thaw cycles (Calcium Chloride solution was used in both cases) and graphite reinforced beams as the most durable compared to aramid and E-glass reinforced beams (36 % drop in strength was observed for aramid and E-glass reinforced beams due to wet–dry cycles). Toutanji and Gómez (1997) also observed reduction of strength of two types of FRP-strengthened beams due to wet–dry cycles of salt water. The performance of CFRP-strengthened beams was better than GFRP-strengthened beams. Myers et al. (2001) investigated the combined effect of freeze–thaw cycles, extreme temperature cycles, relative humidity cycles and indirect ultra-violet radiation exposure under sustained load (0, 25 and 40 % of the ultimate load) on three types of FRP (Carbon, Glass and Aramid)-concrete bond by means of four point bending tests of pre-cracked reinforced concrete (RC) beams. They reported the degradation of flexural stiffness due to environmental conditions, especially for 40 % sustained loads. GFRP (Glass Fibre Reinforced) strengthened beams showed the highest stiffness degradation (about 85 %). This study mainly considered the comparison of strain profiles and flexural stiffness at a reference load level 60 % of the ultimate load. In a similar study, Li et al.

<sup>1)</sup>Institute for Infrastructure Engineering, Western Sydney University, Kingswood, NSW 2747, Australia.

\*Corresponding Author;

E-mail: ikramulkabir@gmail.com

<sup>2)</sup>Centre for Built Infrastructure Research, University of Technology Sydney, Ultimo, NSW 2007, Australia.

Copyright © The Author(s) 2016. This article is published with open access at Springerlink.com

(2002) strengthened pre-cracked RC beams with carbon fibre reinforced polymer (CFRP) and GFRP sheets and investigated the combined effect of boiling water and UV-light. Test results showed 57–76 % loss of strengthening efficiency and 43–48 % loss of stiffness due to exposure. Unlike other studies, this study observed that CFRP-strengthened beams did not show higher remaining increase in strength than GFRP-strengthened beams after the exposure duration although CFRP is well known for its more durable performance than GFRP. The reason was attributed to the deterioration of epoxy resin, and fibres, therefore, only had a secondary role. Grace (2004) investigated the effects of six types of environmental conditions on CFRP-strengthened concrete beams and reported the highest degradation due to constant 100 % humidity at about 38 °C constant temperature for the duration of 10,000 h. The primary mode of failure of CFRP strengthened beams with or without exposure was debonding of CFRP. This type of failure mode observed requires quantification of bond strength due to exposure conditions by means of appropriate test set-up. Research conducted by Homam et al. (2001), Dai et al. (2010), Benzarti et al. (2011), Yun and Wu (2011) and Imani et al. (2010) focused on the performance of FRP-concrete bond system under freeze–thaw cycles, temperature cycles, alkali solutions, moisture ingress, hydrothermal ageing with the help of various test set-ups such as pull-off, bend tests, single-lap-joint shear tests, etc. Peel and shear fracture tests were used by Tuakta and Büyüköztürk (2011) to study the effect of moisture on FRP-concrete bond system by tri-layer fracture mechanics. Benzarti et al. (2011) observed the sensitivity of single shear test (pull-out test) to environmental conditions and suggested the use of the set-up for adhesive bonded joints. In addition, Imani et al. (2010) adopted this test method because debonding of externally bonded FRP mainly occurs due to Mode II (shear) fracture. Moreover, according to Teng et al. (2002), this set-up can simulate an important failure mode (intermediate flexural crack-induced debonding) of reinforced concrete beams strengthened with FRP. Although this failure mode occurs due to both shear and normal stress, shear stress is the dominant one in this type of failure and, therefore, can be simulated by direct shear test. Hence, more research applying the test set-up can be helpful to create a large database of FRP-concrete bond behaviour under various environmental conditions.

Research studies by Litherland et al. (1981), Dejke and Tepfers (2001) and Phani and Bose (1987) proposed long term prediction models for FRP and FRP in concrete environment applying high temperature to accelerate degradation rate. Their studies mainly investigated the durability of FRP not the bond between FRP and concrete. Arrhenius Principle was adopted in their research for acceleration of chemical reaction rate. However, According to Robert et al. (2010), the use of high temperature may amplify the reduction of the properties, leading to conservative prediction of long-term properties. This inherent conservativeness necessitates further research by separating the high temperature from a specific degradation mechanism.

Very limited data of natural ageing of FRP-concrete bond is another aspect found in the available literature and should be addressed accordingly. Nishizaki and Kato (2011) investigated the durability of CFRP-concrete bond exposed to outdoor environment of Tsukuba Japan (moderate climate) for 14 years since 1992 by means of pull-off and peel tests. Slight reduction of pull-off strength was observed after 14 years of exposure but the peel test showed much deviation of strength due to outdoor environment and change of failure modes. However, the results of peel tests were not conclusive because the unexposed specimens of this series were fabricated much later (in 2006) than 1992 and could not be made from exactly the same materials used in 1992. Al-Tamimi et al. (2014) investigated the effect of dry exposure to sun as well as the saline water coupled with exposure to sun on CFRP-concrete bond specimens for more than 150 days. In both conditions, sustained loads of 15 and 25 % were used. The outdoor environment was chosen as summer time environment (temperature stays within the range between 38 and 55 °C at least for 3 months) of United Arab Emirates (UAE). Single shear tests were used to measure the bond strength after the exposure duration. The test results showed that harsh environment increased the bond strengths and the reason was attributed to greater polymer cross-linking due to elevated temperature. The interesting findings of the available two studies clearly reflect the need for further research on natural ageing of FRP-concrete bond in different climatic regimes.

The current research aims to investigate the effects of temperature cycles, humidity cycles and outdoor environment separately on CFRP-concrete and GFRP-concrete bond using single shear test (pull-out test) for up to 18 months. This paper only presents the experimental results of GFRP bonded specimens, whereas the same for CFRP-concrete bond can be found in the PhD thesis by Kabir (2014) and Kabir et al. (2016a). The results of compressive tests on concrete cylinders subjected to the same environmental conditions are also discussed to understand the effect of concrete compressive strengths on the changing behaviour of GFRP-concrete bond.

## 2. Experimental Program

Single shear tests (referred to as pull-out test herein) were used to determine the strength of GFRP-concrete bond specimens exposed to three different environmental conditions (temperature cycles, wet–dry cycles and outdoor environment) for durations up to 18 months. In addition, concrete cylinders were fabricated from the same concrete mix used for pull-out specimens and were exposed to the same environmental conditions in order to identify the compressive strength of concrete on the day of each pull-out test.

### 2.1 Pull-out Test of GFRP-Concrete Bond Specimens

#### 2.1.1 Specimen Geometry

GFRP pull-out specimens consisted of a concrete prism with dimensions of 300 mm × 200 mm × 150 mm and

two layers of 40 mm wide FRP strip were bonded to the top of concrete prism. The total length of GFRP was 400 mm, including the bond length of 150 mm (Fig. 1). The bond length of 150 mm was selected in a manner to satisfy the effective bond length (84.5 mm) measured by the Eq. (1) recommended by Chen and Teng (2001). Effective bond length can be defined as the active length for transferring of most of the interfacial stress from FRP sheets to concrete and beyond this length failure load does not increase (Ouezdou et al. 2009; Kang et al. 2012). The bond length much longer than the effective bond length was chosen considering the possibility of increase in effective bond length due to environmental conditions and to keep the provision for the development of the full capacity of bond in that case.

$$L_e = \sqrt{\frac{E_f t_f}{\sqrt{f'_c}}} \quad (1)$$

where  $L_e$  = effective bond length,  $E_f$  = tensile modulus of elasticity of FRP,  $t_f$  = thickness of FRP and  $f'_c$  = compressive strength of concrete.

A gap of 50 mm was provided between the loaded edge of adhesive bonded joint and concrete edge to prevent the edge or boundary effect and to avoid wedge (triangular section) failure in concrete prism (Mazzotti et al. 2008, 2009). The FRP strip was extended to 200 mm beyond the concrete prism to facilitate gripping by the jaws of the testing machine.

### 2.1.2 Fabrication of Pull-out Specimens and Materials Properties

After concrete prisms were fabricated, moist curing was conducted for 7 days by sprinkling water regularly and covering them with plastic sheets. Then concrete specimens were air cured under laboratory environment (22–23 °C temperature and 61–63 % relative humidity) for three more weeks. After 28 days (moist and air curing), surface preparation was conducted by exposing the aggregates by needle-gun. Two plies of GFRP strip were externally bonded to the concrete prism with two part epoxy impregnation resin. In addition, concrete cylinders were cast to determine compressive properties of unexposed and exposed cylinders according to Australian Standards (AS 1012.9 1999; AS

1012.17 1997). Cylinders were also cured using the same condition as used for the prisms. Moreover, GFRP coupons were prepared as per ASTM D3039/D3039M (2008) to investigate the tensile properties of GFRP only for unexposed condition. The properties of concrete measured at 28 days are shown in Table 1 whereas Table 2 provides the properties of GFRP and epoxy resin.

### 2.1.3 Exposure Conditions

**2.1.3.1 Control Specimens** Five specimens were used as control specimens (GControl-1 to 5; where G refers to Glass and numbers from 1 to 5 refer to the specimen number). After fabrication, control specimens were kept under lab conditions (22–23 °C temperature and 61–63 % relative humidity) for curing of wet lay-up GFRP for 7 days before they were tested under pull-out load.

**2.1.3.2 Exposed Specimens** The remaining specimens were subjected to three types of exposure conditions—(1) temperature cycles (2) wet–dry cycles and (3) outdoor environment as shown in Figs. 2, 3 and 4, respectively after curing of FRP for 7 days.

Typical temperature cycle (Fig. 2b) consisted of very sharp rise to 40 °C from 30 °C within 3 min, constant 40 °C for 4 h and 57 min and a gradual decrease to 30° C and two cycles per day were maintained. The reason for using the cyclic temperature instead of constant temperature was to simulate the effect of natural fluctuation in temperature. Total of nine specimens were used for this cyclic temperature series and specimens were exposed to 70 cycles (35 days), referred to as GT2 series, 180 cycles (90 days), referred to as GT3 and 730 cycles (1 year), referred to as GT4 series.

The wet–dry cycles consisted of 1 week wetting followed by 1 week drying and at least 95 % RH was maintained for wetting. Wet–dry cycles were chosen for this current study to simulate the variation in air relative humidity and thereby subjecting the GFRP-concrete bond to cyclic moisture absorption and desorption. The 1 week time both for wetting and drying process was selected to allow the specimens to gain and loose sufficient amount of moisture. Although the main aim was to maintain constant temperature during wet and dry cycles, steam generated from humidifier raised the

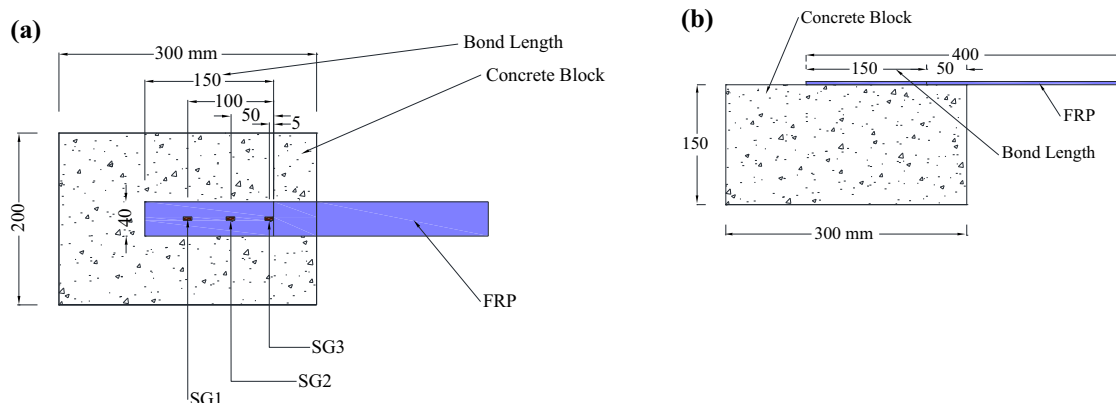


Fig. 1 Geometry of pull-out specimens. a plan, b elevation.

**Table 1** Properties of concrete.

Concrete Batch	Target compressive strength (MPa)	Measured 28 days cylinder compressive strength (MPa)	Maximum aggregate size (mm)
2	32	42.0	10

**Table 2** Mechanical properties of GFRP and epoxy resin.

Material name	Mechanical properties			
GFRP (MBRACE EG 90/10A)	Thickness per ply	Measured tensile strength		Measured tensile modulus of elasticity
	(mm)	(MPa)		(GPa)
	0.154	1,657		139
Epoxy <sup>a</sup>	Tensile strength after 7 days of curing at + 23 °C	Tensile modulus of elasticity after 7 days of curing at + 23 °C	Coefficient of thermal expansion between - 10° C to + 40 °C	Heat distortion/ glass transition temperature (T <sub>g</sub> ) after 7 days of curing at + 23 °C
	(MPa)	(GPa)	(/°C)	(°C)
	30	4.5	$4.5 \times 10^{-5}$	+ 47

<sup>a</sup> The properties of epoxy resin are according to the supplier's information.

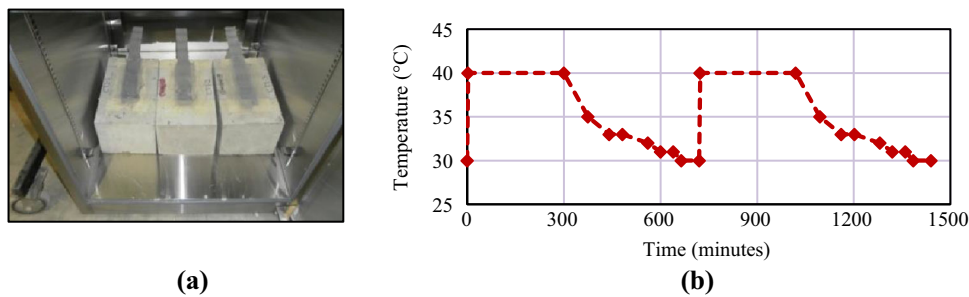


**Fig. 2** a Specimens in drying oven and b temperature cycles.

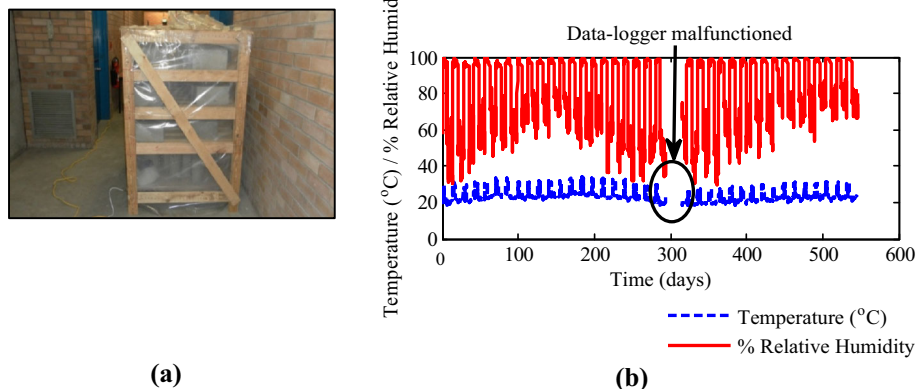


**Fig. 3** a Humidity chamber and b wet-dry cycles with corresponding temperature.

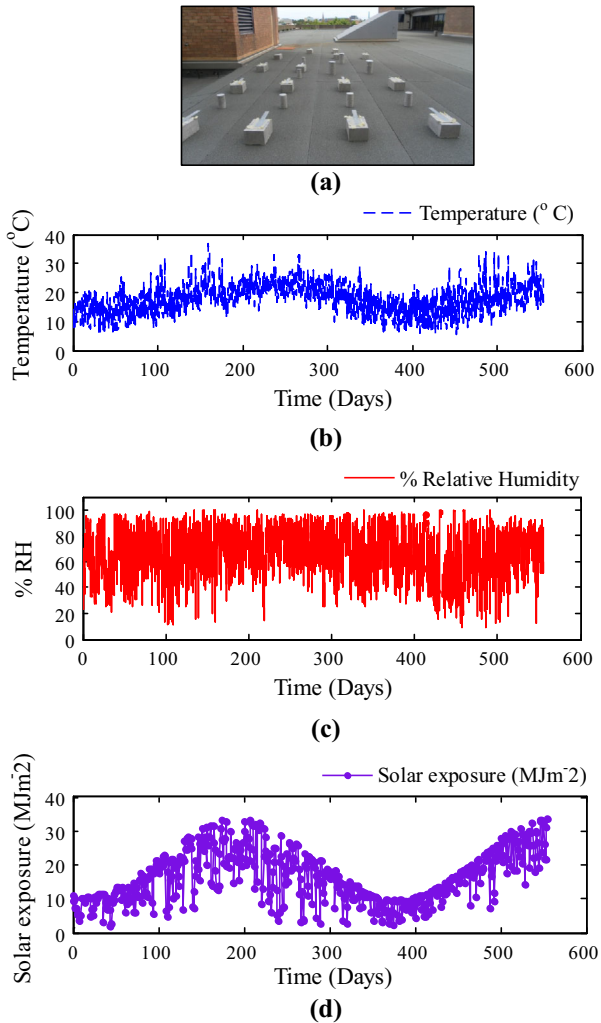


**Fig. 4** Outdoor environment and three environmental parameters for outdoor environmental exposure. **a** specimens under outdoor environment, **b** temperature plot (Sydney Observatory Hill), **c** % relative humidity plot (Sydney Observatory Hill), **d** solar exposure plot (Sydney Observatory Hill). *Source:* Australian Government Bureau of Meteorology.

temperature to about 30–32 °C during wetting (the peak of the temperature plot in Fig. 3b). The temperature was almost constant in the range of 20–23 °C during drying period. The relative humidity during drying depended on the lab environment and showed scatters between 30 and 70 %. Humidity specimens were subjected to wet–dry cycles for 1 month (GH1 series), 6 months (GH2 series), 12 months (GH3 series) and 18 months (GH4 series).

A more detailed explanation of how the protocols of temperature cycles and wet–dry cycles were selected can be found in the study by Kabir et al. (2016b).

A number of specimens were directly exposed to outdoor environment of Sydney, Australia for 2 months (GE1 series), 6 months (GE2 series), 12 months (GE3 series) and 18 months (GE4 series). Some of the environmental parameters, namely, temperature, relative humidity and solar exposure data collected from Australian Government Bureau of Meteorology are plotted against time (from June, 2011 to December, 2012) in Fig. 4. The environmental parameters were measured at the data

station at Sydney Observatory Hill, which is only about 2 km from the location of the exposed specimens.

In the nomenclature of the specimens, the first letter, G, represents GFRP; the second letter represents the exposure condition (T-temperature, H-humid environment/wet–dry cycles and E-outdoor environment); the first number refers to the exposure period, i.e.; 1st, 2nd, 3rd or 4th; and the last number represents the serial number of specimen. For temperature specimens, the first letter however starts from 2 as a number of specimens were fabricated in order to study the effect of constant temperature and named as GT1 series but discarded later from the experimental study. The number of specimens exposed to each condition is listed in Table 3.

#### 2.1.4 Test Set-Up and Instrumentation

A universal testing machine with 500 kN loading capacity was used for the pull-out test. The testing machine was operated with the maximum load range of 20 kN as the predicted load capacity [determined from Chen and Teng (2001) model] for control series was within this range. The pull-out test set-up is shown in Fig. 5. A linear variable differential transformer (LVDT) was used to measure the cross head travel of lower fixed head of the machine. A data taker was used for continuous recording of load, strain and cross head travel data. In order to acquire strain profile along the bonded GFRP, three-four strain gauges with 10 mm gauge length and  $119.9 \pm 0.1$  Ohms resistance were glued to the GFRP surface.

#### 2.1.5 Experimental Procedure

After individual specimens were placed on a plate fixed to the lower cross head and restrained with two bolts and top plate (Fig. 5), pull-out test was performed with a loading (tensile load) rate of approximately 2 mm/min in terms of cross-head travel of the testing machine. The loading rate was selected as per ASTM D3039/D3039M (2008) due to the absence of standard method for pull-out test. The cross head displacement was constantly monitored and the load rate was adjusted to maintain the constant displacement of cross head. The load was applied monotonically until failure and gathered data were analysed in terms of maximum load, strain profiles and failure modes. The maximum load of failure was converted to the maximum axial stress developed in FRP using Eq. (2):

$$\sigma_{db} = \frac{P_{max}}{b_f t_f} \quad (2)$$

where  $\sigma_{db}$  = maximum axial stress on FRP sheet at debonding in MPa,  $P_{max}$  = maximum load of debonding,  $b_f$  = width of FRP sheet and  $t_f$  = thickness of FRP sheet.

### 3. Test Results and Discussion

The test results of both control and exposed GFRP pull-out specimens are presented in terms of pull-out strengths, failure modes and strain profiles. The change of bond behaviour due to environmental conditions is discussed as comparison of exposed series with control series for each applied condition.

**Table 3** Number of pull-out specimens.

Exposure condition	Number of specimens	Name of specimens	Exposure period
Control	5	GControl-1 to 5	–
Temperature cycle <sup>a</sup>	3	GT2-1 to 3	5 weeks
Wet–dry cycle <sup>b</sup>	5	GH1-1 to 5	1 month
Outdoor environment	5	GE1-1 to 5	2 months
Temperature cycle <sup>a</sup>	3	GT3-1 to 3	3 months
Wet–dry cycle <sup>b</sup>	5	GH2-1 to 5	6 months
Outdoor environment	5	GE2-1 to 5	6 months
Temperature cycle <sup>a</sup>	3	GT4-1 to 3	12 months
Wet–dry cycle <sup>b</sup>	5	GH3-1 to 5	12 months
Outdoor environment	5	GE3-1 to 5	12 months
Wet–dry cycle <sup>b</sup>	5	GH4-1 to 5	18 months
Outdoor environment	5	GE4-1 to 5	18 months
Total number of specimens	54		

<sup>a</sup> 5 h at constant 40 °C followed by 7 h at gradual decrease to 30 °C.

<sup>b</sup> 1 week at around 95 % RH followed by 1 week at normal lab condition.

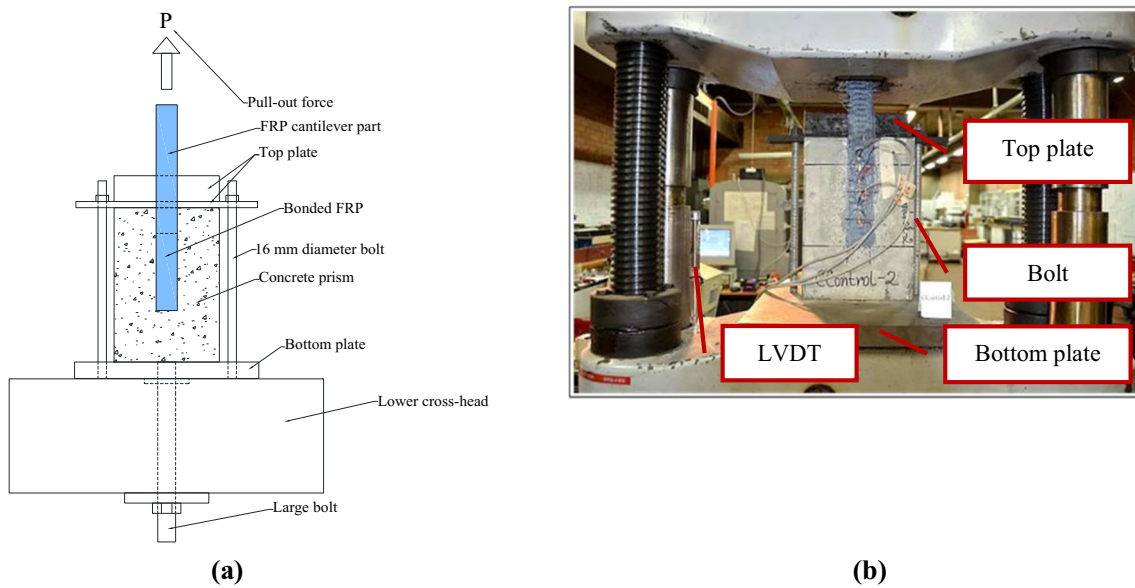


**Fig. 5** Pull-out test set-up: **a** schematic diagram and **b** photograph.

### 3.1 Pull-out Strengths

#### 3.1.1 Control Series

A total of five control-GFRP bonded prisms were tested under direct shear tests and the maximum axial stress

developed in GFRP before debonding was considered as pull-out strength of each specimen. The average maximum stress developed in GFRP before debonding was 1027 MPa with a coefficient of variation (CoV) of 6 %.

**Table 4** GFRP pull-out strengths of cyclic temperature specimens.

Exposure duration (days)	Mean pull-out strength (MPa)	CoV of pull-out strength (%)
0	1027	6.0
35	1056	5.5
90	1065	1.9
365	1113	1.7

**Table 5** GFRP pull-out strengths of wet-dry specimens.

Exposure duration (days)	Mean pull-out strength (MPa)	CoV of pull-out strength (%)
0	1027	6.0
28	1022	10.8
168	961	12.4
364	1011	6.9
546	1034	5.0

**Table 6** Pull-out strengths of GFRP outdoor environment specimens.

Exposure duration (days)	Mean pull-out strength (MPa)	CoV of pull-out strength (%)
0	1027	6.0
60	941	7.0
180	931	6.3
365	970	7.0
555	1023	6.3

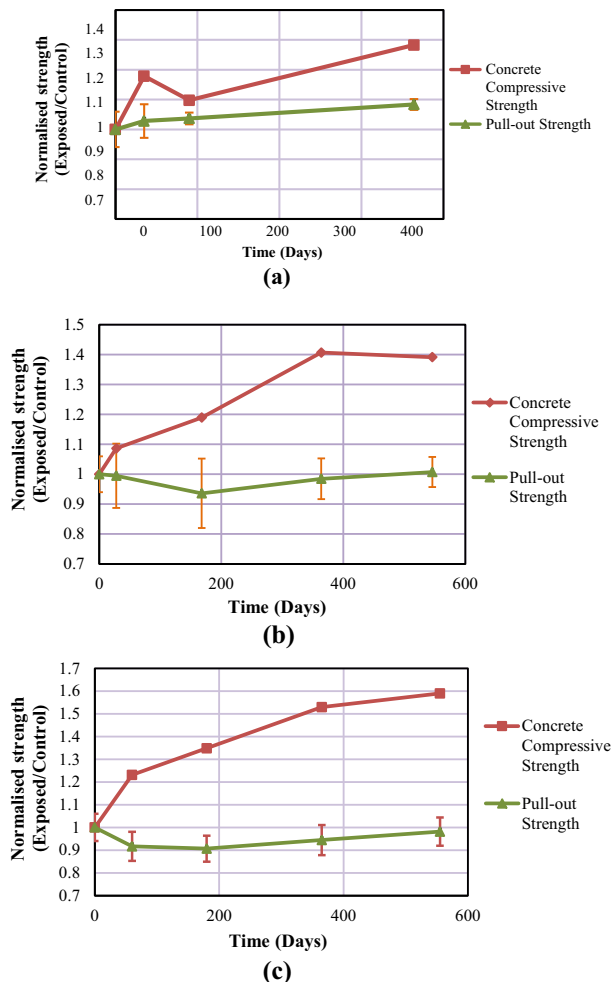


**Fig. 6** Normalised pull-out strength against exposure duration: **a** temperature cycles, **b** wet-dry cycles and **c** outdoor environment.

### 3.1.2 Exposed Series

Average pull-out strengths of temperature cycles, wet-dry cycles and outdoor environment series are listed in Tables 4, 5 and 6, respectively whereas the change of normalised average pull-out strength (expressed as the ratio of exposed strength to unexposed/control strength) with exposure duration is illustrated in Fig. 6. The vertical bars in the graphs represent the CoV for the normalised average pull-out strength. In addition, the change of normalised concrete compressive strength with exposure duration is shown in the same figure.

#### 3.1.2.1 Temperature Cycles

From Fig. 6a, continuous increase in mean pull-out strength (bond strength) is clearly visible. The increase in bond strength was by about 3 % after 5 weeks compared to the control strength and then bond strength increased gradually until it reaches about 8 % more than the control value at the end of the 1 year exposure. From the observations, it can be stated that the cyclic temperature did not cause any negative effect on pull-out strength of the GFRP specimens even after 1 year of exposure; rather it improved the strength during the whole exposure period. The increase in bond strength can be correlated with the increased compressive strength as shown in the same figure. Although a decreasing trend of concrete compressive strength was visible after 3 months, the strength value was always more than that of the control series. The gradual increase in pull-out strength after 3 months may be attributed to the decreasing trend of the concrete compressive strength.

#### 3.1.2.2 Wet-Dry Cycles

From Fig. 6b, it is seen that wet-dry series degraded the performance of GFRP-concrete bond by about 6.4 % compared to the control series after the exposure for 6 months although the concrete compressive

strength increased. Then, an increasing trend of pull-out strength was observed with the strength value reaching the control strength after 18 months. Therefore, the maximum deterioration of GFRP-concrete pull-out strength observed in this study was only 6.4 %. On the other hand, the concrete compressive strength was found to increase continuously up to 1 year and then became almost constant.

**3.1.2.3 Outdoor Environment** Outdoor environment series showed an initial reduction of the pull-out strength (to 90.7 % after 6 months) followed by a recovery in the pull-out strength reaching to 98.2 % of the control value after 18 months (Fig. 6c). On the other hand, concrete compressive strength increased continuously with time during the whole exposure duration of 18 months. The reason for the degradation of pull-out strength despite the increase in concrete compressive strength is discussed later through observed failure modes.

### 3.2 Failure Modes

The modes of failure of control series and exposed series, namely, temperature cycles, wet-dry cycles and outdoor environment series are presented in this section.

#### 3.2.1 Control Series

The failure modes observed after testing of control series were mainly associated with thick concrete layer attached to debonded GFRP. Most specimens failed in concrete substrate with the exception of GControl-4 which had a very thin layer of concrete as well as visible epoxy layer attached to the debonded GFRP coupon. The typical failure pattern of this series is shown in Fig. 7a whereas the failure mode of GControl-4 is given in Fig. 7b.

#### 3.2.2 Temperature Cycles

Figure 8 illustrates the failure modes of GFRP cyclic temperature series.

Specimens of five week temperature (GT2) series failed with very thick concrete layer attached to the debonded GFRP (Fig. 8a).

GT3 (3 months temperature) series and GT4 series (Fig. 8b, c, respectively) showed almost similar pattern of failure to GT2 series.

From the comparison of failure modes of all temperature series (Fig. 8) with the control series (Fig. 7), the change of

failure patterns with duration of exposure deemed to be insignificant as the failure always occurred mostly in the concrete adjacent to the epoxy layer.

#### 3.2.3 Wet-Dry Cycles

One month wet-dry (GH1) series showed failure of specimens with very thin layer of concrete attached to debonded GFRP (Fig. 9a) and the pattern was identified as failure in the interface between epoxy and concrete.

Six months wet-dry (GH2) series showed similar pattern of failure to that observed in GH1 series. The thickness of attached concrete on GFRP, although slightly more than GH1 series, was much less than the control series. Moreover, epoxy layer was visible in many parts of the debonded GFRP coupons (Fig. 9b).

Most specimens from 1 year wet-dry (GH3) series exhibited thin concrete layer on debonded GFRP (Fig. 9c).

Eighteen months wet-dry series (GH4) experienced change of failure modes from thin concrete to thicker concrete layer attached to the debonded FRP. Most specimens showed this type of failure as illustrated in Fig. 9d.

In summary, evolution of failure modes from thick concrete layer attached to debonded GFRP in control series to thinner/very thin layer in exposed series was observed in this study. Only the 18 months wet-dry series (GH4) showed almost similar mode of failure to that of control series.

#### 3.2.4 Outdoor Environment

Two months outdoor environment (GE1) series showed shifting of failure modes from thick layer of concrete to very thin layer of concrete attached to debonded GFRP in comparison with the GFRP control specimens. In fact, visual inspection (Fig. 10a) confirmed that the failure mainly occurred in hardened cement paste adjacent to the epoxy layer. The epoxy layer was visible on most part of the concrete substrate and debonded GFRP.

Similar to GE1 series, 6 months (GE2) series also exhibited failure modes with almost no concrete attached to GFRP (Fig. 10b).

One year (GE3) series had almost no concrete attached to debonded FRP. In addition, mostly, epoxy was visible all over the debonded GFRP strip as illustrated in Fig. 10c.

In 18 month (GE4) series, failure mode similar to GE3 series was observed (Fig. 10d).

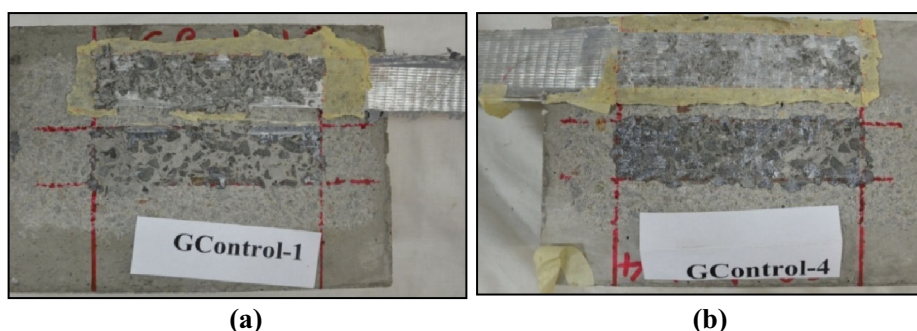
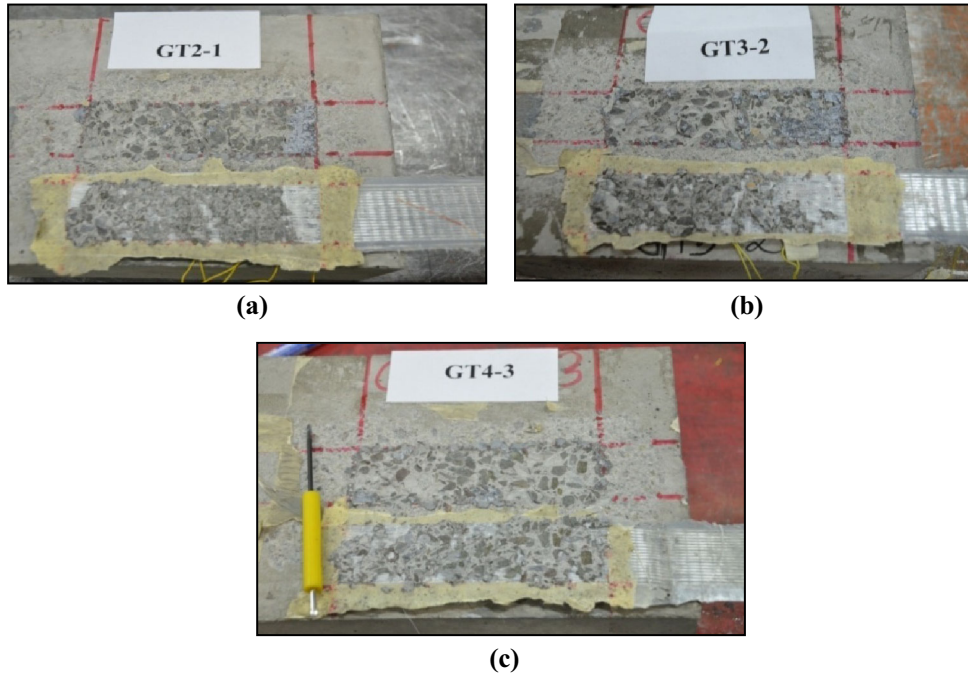
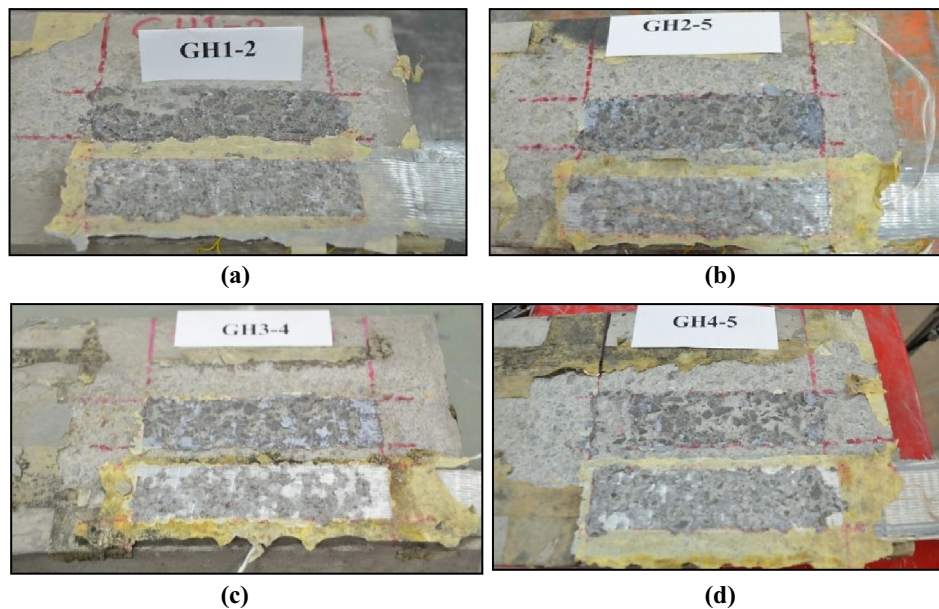


Fig. 7 Failure modes of GFRP control pull-out specimens. a GControl-1, b GControl-4.



**Fig. 8** Failure modes of GFRP cyclic temperature specimens. **a** GT2-1, **b** GT3-2, **c** GT4-3.



**Fig. 9** Failure modes of GFRP wet-dry specimens. **a** GH1-2, **b** GH2-5, **c** GH3-4, **d** GH4-5

Based on failure patterns of all GFRP outdoor environment series, it can be summarised that exposed condition changed the mode of failure from very thick concrete layer to very thin concrete layer attached to GFRP coupon compared to control series. Especially, GE3 and GE4 series showed hardly any concrete attached to debonded GFRP. Hence, the failure modes for all series can be assumed as adhesive-concrete interfacial failure.

### 3.3 Strain Profiles

The strain distribution diagrams (*referred to as strain profiles from here onwards*) along the bond length were plotted mostly based on the readings of three strain gauges

(Fig. 11) at different levels of loads to understand the stress transfer lengths and effective bond lengths of the specimens. The distances of three strain gauges were measured from the loaded end as 5, 50 and 100 mm. According to Bizindavyi and Neale (1999), the stress transfer length can be defined as the length along the bond line from the loading point to the point at which strain becomes zero. The stress transfer length maintains a constant value until a crack forms and this transfer length is referred to as initial stress transfer length. With the progression of cracks, stress transfer length changes.

Effective bond length (the bond length requires to achieve the maximum bond strength) was determined by observing

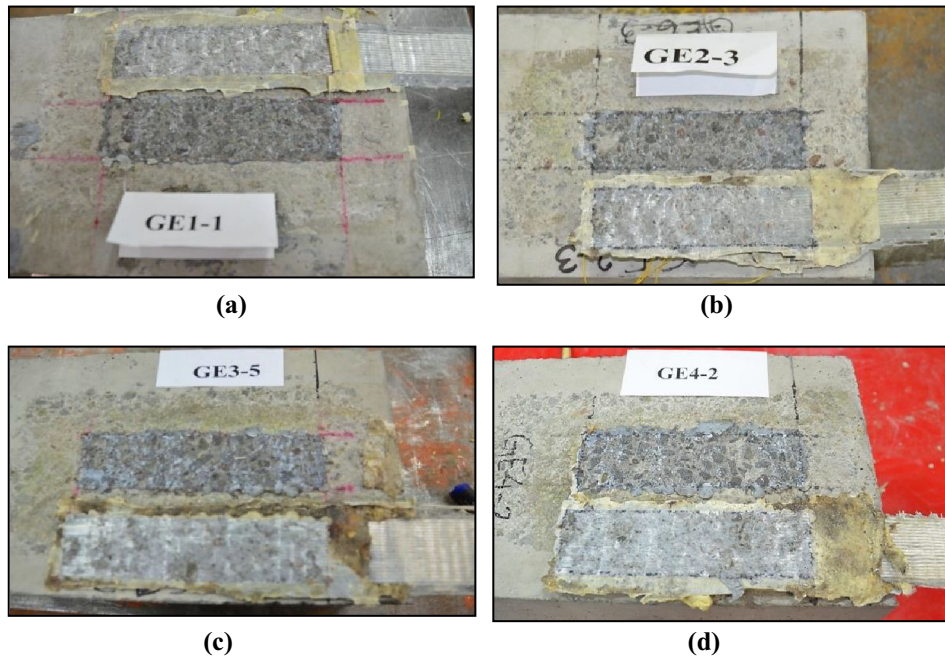


**Fig. 10** Failure modes of GFRP outdoor environment specimens. a GE1-1, b GE2-1, c GE3-5, d GE4-2.

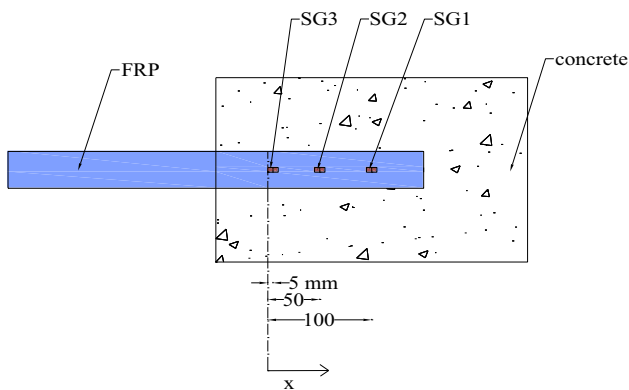


**Fig. 11** Typical strain gauge locations.

the stress transfer length either at 97 % of ultimate load (Yuan et al. 2004) or at 99 % of ultimate load (Lu et al. 2005). The comparison of effective bond lengths of exposed specimens with those of control specimens are presented later in this paper to investigate the effect of environmental conditions on the effective bond length. It should be noted that the stress transfer lengths and effective bond lengths measured based on the limited number of strain gauges with large intervals applied in this study are unlikely to represent true lengths. However, comparison of strain profiles of exposed and control series can still provide information regarding the changing nature of the stress transfer and effective bond lengths. Further studies employing more strain gauges with close intervals should be conducted to estimate the effective bond lengths accurately.

### 3.3.1 Control Series

Strains for control GFRP specimens were observed to be distributed mainly at 0–50 mm location until load value reached very close to the maximum (Fig. 12). Almost all

specimens showed stress transfer length (initial transfer length) of approximately 50 mm except when the load reached close to the maximum pull-out forces. The change of initial stress transfer lengths of GFRP specimens from 50 to 100 mm were observed at 11–12.6 kN. Most specimens showed effective bond length of 100 mm or less according to the definition of effective bond length as the load transfer length either at 97 % or at 99 % of the maximum load in pull-out test. The effective bond length calculated using Chen and Teng (2001) model was 84.5 mm which was close to the experimental effective bond lengths.

### 3.3.2 Temperature Cycles

The strain profiles for GT2 and GT3 series were obtained by three strain gauge set-ups (Fig. 11), and those for GT4 series were obtained by four strain gauge set-ups (Fig. 13).

In GT2 series (Fig. 14a) the initial stress transfer length of about 50 mm remained unchanged until the load reached close to the ultimate load. The change of initial transfer length approximately from 50 mm to 100 mm occurred at 10–12 kN load for this series. The behaviour of strain profiles of GT2 series was almost similar to that found in GFRP control series. The effective bond length can be assumed from the definitions by Yuan et al. (2004) and Lu et al. (2005) as more than 100 mm. Therefore, the change of effective bond length can be observed when compared to the experimental effective bond length (100 mm or less) of control series.

As illustrated in Fig. 14b, strain profiles of GT3 series were similar to the control and GT2 series. The initial stress transfer length shifted at 11–13 kN load. The experimental effective bond length can be considered as more than 100 mm and are exactly as same as those with 5 weeks temperature series.

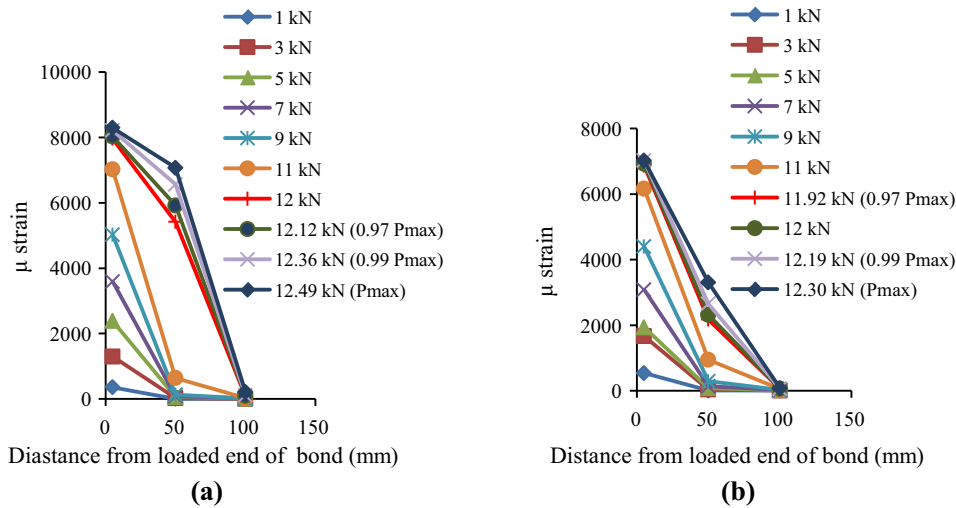


Fig. 12 Strain profiles of GFRP control pull-out specimens. a GControl-1, b GControl-5.

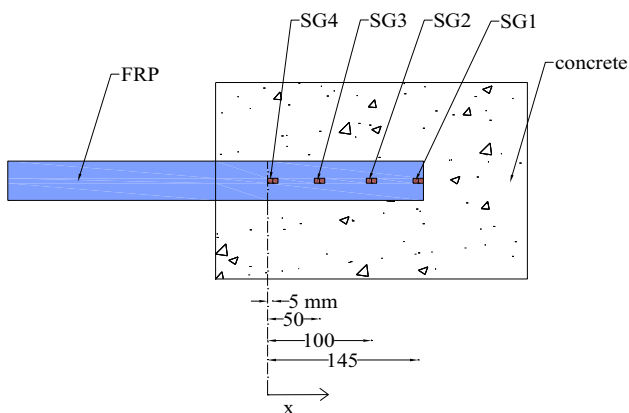


Fig. 13 Four strain gauge setup.

GT4 series (Fig. 14c) experienced the change of stress transfer length after the load value reached about 10 kN. Based on the definitions of effective bond length by Yuan et al. (2004) and Lu et al. (2005), all specimens from one year series had effective bond length of more than 100 mm.

It can be summarised that although the overall behaviour of strain profiles were quite similar to the control series in terms of the load levels for shifting of initial stress transfer lengths, the effective bond length exceeded 100 mm which is longer than that in control series. Hence, for the achievement of full capacity of GFRP-concrete bond in long term, longer bond length than the effective bond length for unexposed condition is required.

### 3.3.3 Wet-Dry Cycles

The strain profiles of GH1 and GH2 series were plotted for three strain gauge set-up (Fig. 11), whereas those for GH3 and GH4 series were plotted for four strain gauge set-up (Fig. 13)

Strain profiles of GH1 series (Fig. 15a) were almost similar to those of control series (Fig. 12). The initial stress transfer length changed from approximately 50–100 mm at load level of 9–11 kN which was slightly lower than control

series. The effective bond lengths were 100 mm or less by the definitions of Yuan et al. (2004) and Lu et al. (2005), which was similar to the control series.

The initial transfer length of GH2 series (Fig. 15b) was observed to change at relatively lower load level than control series as the load level was 8–10 kN. In terms of effective bond length, most specimens showed similar length to that of control series; i.e. 100 mm or less.

In GH3 series (Fig. 15c), the change of initial stress transfer length occurred at about 10–12 kN load. Hence, the overall behaviour of the strain distributions, in terms of initial stress transfer length, was almost similar to that of control series, although the load level for the shifting of initial transfer length was slightly lower than the control series. However, the effective bond lengths were found to be more than 100 mm which was higher than those obtained from control series.

GH4 series (Fig. 15d), although showed higher effective bond lengths (more than 100 mm for most specimens) than control series, the load level at which the change of initial stress transfer length occurred revealed quite a similar pattern. Specimens experienced the shifting of initial transfer length at 11–12 kN.

In summary, the strain distributions of GFRP wet-dry series changed with the exposure duration in terms of level of load at which change of initial stress transfer length occurs and effective bond length.

### 3.3.4 Outdoor Environment

Strain profiles of all series, except GE4 specimens, were plotted for three strain gauge set-up. Only GE4 series had the set-up with four strain gauges.

The strain profile of GE1 series is illustrated in Fig. 16a. The initial stress transfer length changed to approximately 100 mm at loads of 8–10.5 kN. The load levels were found to be lower than the control series. Also, the strain profiles varied from control series in terms of effective bond length as most specimens showed effective bond length of more than 100 mm.

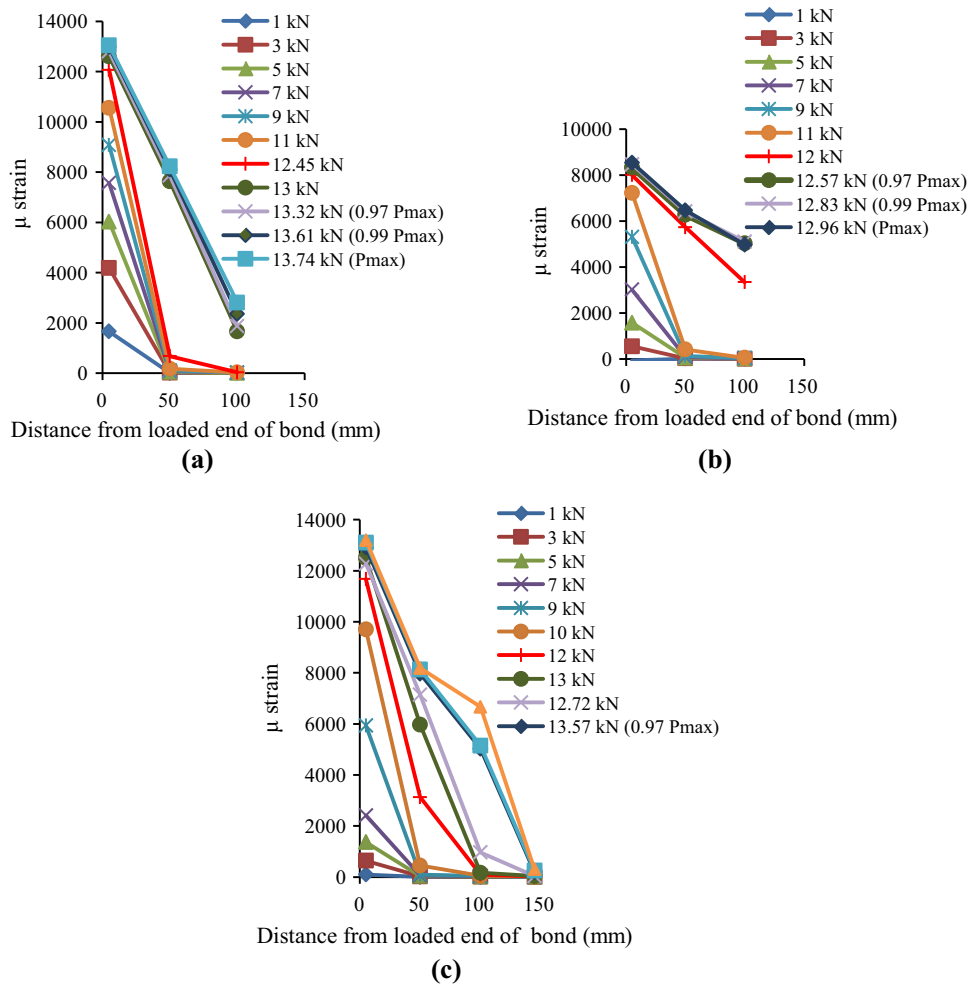


**Fig. 14** Strain profiles of GFRP temperature series. **a** GT2-1, **b** GT3-1, **c** GT4-2.

The strain profile of GE2 series (Fig. 16b), exhibited an interesting behaviour. This series experienced the change of initial transfer length at much lower loads (5–7 kN) than control and GE1 series. Also, the change of strain profiles were gradual with the increase of load and not abrupt (sudden change of transfer length near maximum load) like control series. Similar to GE1 series, GE2 series had effective bond length of more than 100 mm and thereby, differed from the effective bond length of control series.

Unlike the GE2 series, initial transfer length from 50 to 100 mm occurred at higher loads, at 10–11 kN, for GE3 series (Fig. 16c), These loads were slightly lower than that for the control series. However, the effective bond lengths of most of the specimens of this series were more than 100 mm and higher than those observed in control specimens.

The strain profiles of GE4 series were similar to control series in terms of loads (10.5–11 kN) at which shifting of initial transfer length occurred (Fig. 16d). The effective bond lengths can be assumed to be 100 mm at least from the consideration of load transfer length at 97 % of the maximum load.

In summary, strain profiles for GFRP outdoor environment series showed very interesting behaviour in terms of the changes of initial stress transfer lengths. Load at the change

in initial transfer length for GE1 and GE2 were much lower than the control series but this load increased for GE3 and GE4 series, with the load being almost equal to that for control series. This trend exactly coincided with the change of pull-out strength with time of exposure (Fig. 6a). The effective bond lengths for all series, except for GE4, were more than 100 mm.

### 3.4 Discussion

It is obvious from the test results that the temperature cycles did not cause any reduction of pull-out strength for the GFRP specimens. In fact, the temperature cycles helped to improve the strength provided that the highest temperature (40 °C) applied in this study was less than the glass transition temperature of the epoxy resin and the temperature envelope was 30–40 °C. The gaining of bond pull-out strength can be attributed mainly to the increasing concrete compressive strength (Fig. 6) with time as the failure always occurred in the concrete layer adjacent to the epoxy adhesive. The effective bond length obtained from the strain distribution plots suggests that the temperature cycles may increase the bond length in the long term and thereby, using longer bond length may improve the performance of GFRP-concrete bond subjected to such environmental condition.

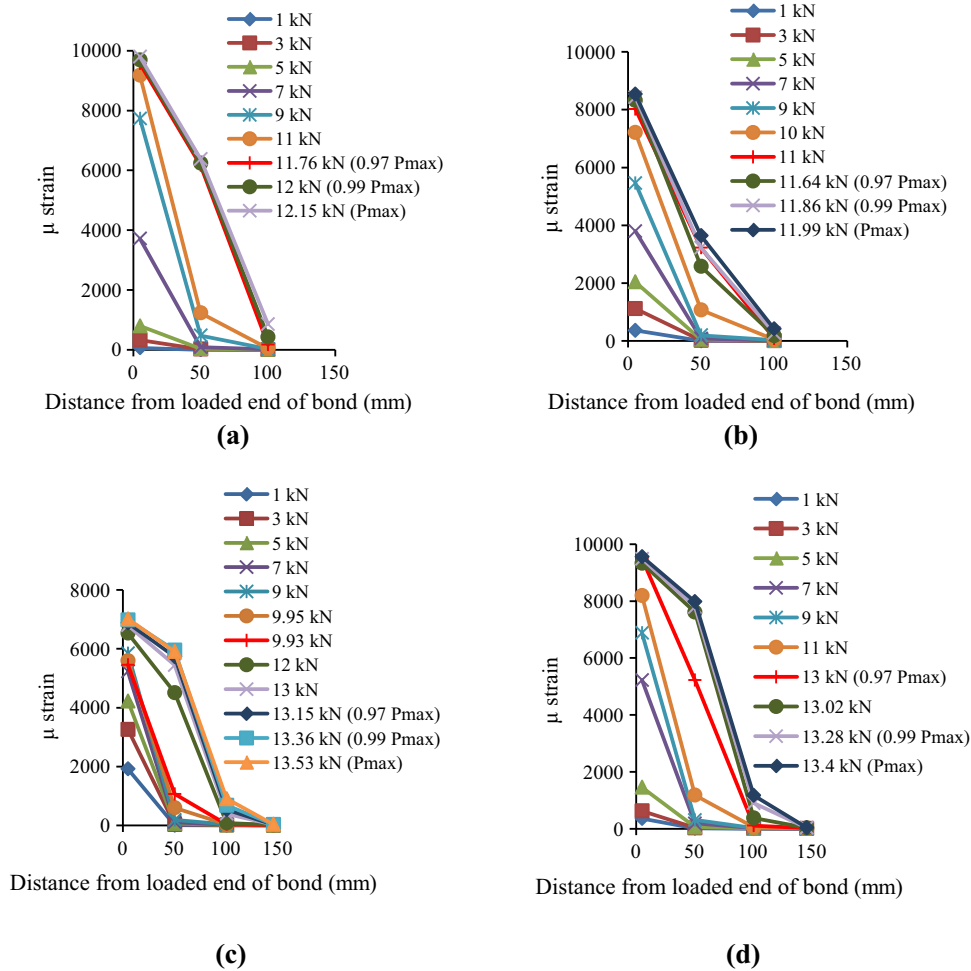


**Fig. 15** Strain profiles of GFRP wet-dry series. **a** GH1-3, **b** GH2-2, **c** GH3-3, **d** GH4-3.

Wet-dry condition had an adverse effect on pull-out strength (although only 6.4 % of reduction) of GFRP-concrete bond. Although the concrete compressive strength increased continuously due to suitable humid condition for the development of concrete strength, the bond strength showed degradation up to 6 months. The degradation can be attributed to the deterioration of epoxy properties (Shrestha et al. 2014) as the failure patterns of pull-out specimens changed from thick concrete to thinner concrete layer attached to GFRP when compared to the control series. Hence, the bond strength was likely to depend more on the epoxy properties than concrete properties. The degradation of epoxy tensile strength (Benzarti et al. 2011), elastic modulus (Benzarti et al. 2011; Tuakta and Büyüköztürk 2011; Shrestha et al. 2014) and shear strength (Shrestha et al. 2014) due to moisture conditions was reported by other studies although the exposure conditions were not as same as the one applied in this paper.

The dependence of bond strength on adhesive properties can also be shown by adopting experimentally developed equations from Dai et al. (2005). In shear tests, the

debonding failure load depends on the maximum interface shear stress,  $\tau_{max}$ . The failure of bond occurs when interface shear stress exceeds the maximum value. Dai et al. (2005) expressed the maximum interface shear stress as follows:

$$\tau_{max} = 0.5BG_f \quad (3)$$

where  $G_f$  is the interfacial fracture energy and  $B$  is an interfacial material constant. These two parameters are related to constituent material properties as shown in Eqs. (4) and (5), respectively.

$$G_f = 0.446 \left( \frac{G_a}{t_a} \right)^{-0.352} f_c^{0.236} (E_f t_f)^{0.023} \quad (4)$$

$$B = 6.846 (E_f t_f)^{0.108} \left( \frac{G_a}{t_a} \right)^{0.833} \quad (5)$$

where  $\frac{G_a}{t_a}$  is shear stiffness of adhesive layer,  $E_f t_f$  is FRP stiffness and  $f_c'$  is concrete compressive strength.

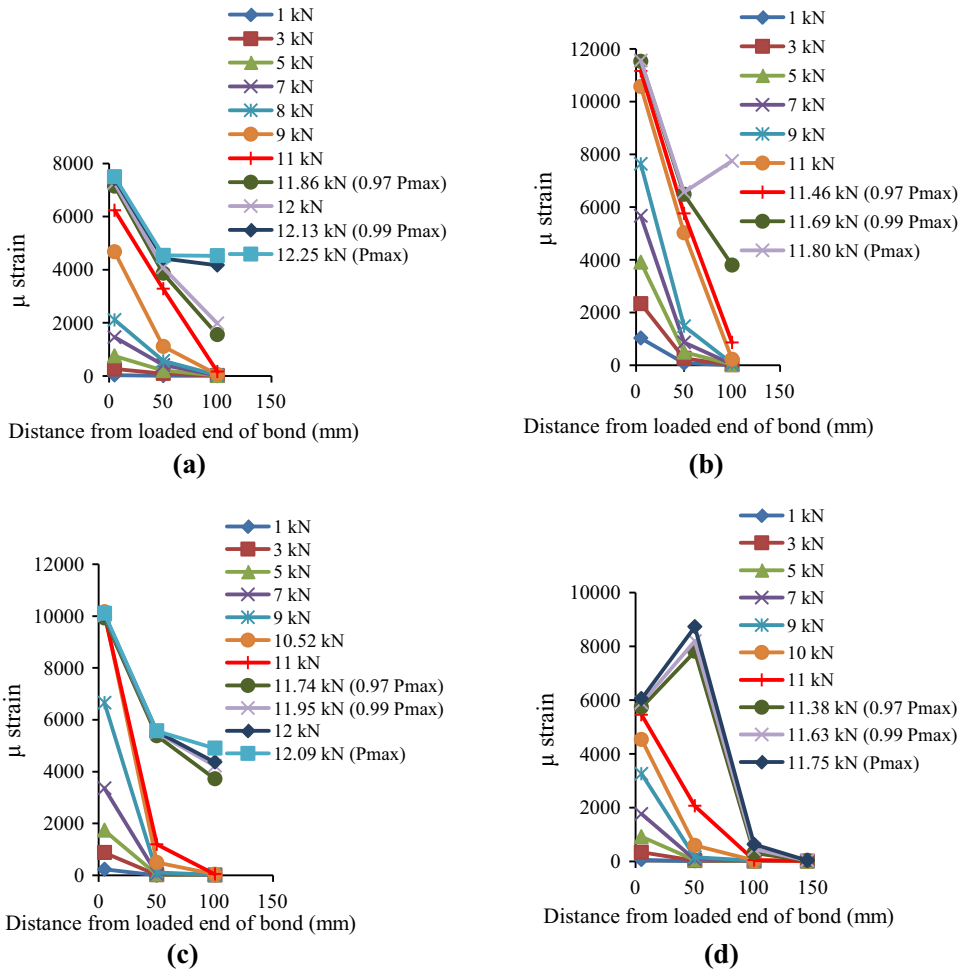


Fig. 16 Strain profiles of GFRP outdoor environment series. a GE1-1, b GE2-1, c GE3-5, d GE4-1.

By substituting Eqs. (4) and (5) into Eq. (3), the expression of maximum interfacial shear stress can be rewritten as

$$\tau_{\max} = 1.527 \left( \frac{G_a}{t_a} \right)^{0.481} f_c^{0.236} (E_f t_f)^{0.131} \quad (6)$$

From Eq. (6), it is obvious that the maximum interfacial shear stress depends on shear stiffness of adhesive layer the most followed by concrete compressive strength, whereas FRP stiffness has the least effect on maximum shear stress. Hence, it is more likely that changed adhesive property due to exposed conditions will affect the bond strength the most.

However, further experimental study on the epoxy properties under the same conditions applied in the current study should be conducted to analyse the concrete-epoxy interface properly and to validate the explanation regarding the dependence of pull-out strength on the epoxy properties.

Since the failure was still in epoxy layer after 1 year of exposure, the significant improvement of pull-out strength can be because of the improved epoxy properties. The approaching of pull-out strength of exposed specimens to the control strength after 18 months of exposure can also be correlated with the failure mode. As the failure pattern of GH4 series was almost similar to the control series (failure

with thick concrete layer attached to GFRP), increased concrete compressive strength helped to improve the bond strength. The change of effective bond length from 100 mm or less to more than 100 mm after one year was noticed in this study and suggests the similar interpretation as for cyclic temperature series.

The pull-out strength of GFRP-concrete bond subjected to outdoor environment was found to deteriorate with time until the maximum degradation of 9.3 % occurred after 6 months. The deterioration of bond can be due to the possible loss of epoxy properties under exposed environment as the concrete compressive strength increased continuously with time. Also, failure modes associated with very thin or almost no concrete attached to debonded GFRP lead to the interpretation that the failure occurred in the adhesive-concrete interface and thereby, epoxy properties had more influence on the bond mechanism than the concrete strength under the exposure of outdoor environment. The gradual improvement of pull-out strength after one year can be attributed to the possible improvement of the epoxy properties as the failure modes were still in the interface. In addition, strain profiles exhibited changing nature with time and the effective bond length increased for exposed specimens compared to control specimens.

## 4. Conclusions

The research findings of this study are highlighted as follows:

### *Temperature cycles*

The temperature cycles did not have any negative effect on the pull-out strength of GFRP-concrete bond. In fact, temperature cycles improved the pull-out strength by 8 % for GFRP-concrete bond. This improvement of pull-out strength is attributed to the increased concrete compressive strength as the failure of bond occurred within the concrete substrate with minimal reduction in concrete thickness.

Strain profiles did not show any changes with the exception of longer effective bond length observed in some exposed series.

### *Wet-dry cycles*

Performance of GFRP-concrete bond under wet-dry cycles was marginally poor (strength reduction by 6.4 % only). The degradation can be attributed to the epoxy degradation as the most series failed with almost no concrete attached to the debonded GFRP.

The trend of the loads at the change of initial stress transfer length also changed with time and followed almost a similar trend to the pull-out strength. Effective bond lengths for most of exposed specimens were longer than that of unexposed specimens for most exposure durations.

### *Outdoor environment*

Exposure to outdoor environment caused the most serious deterioration of pull-out strength (9.3 %). Deterioration of bond strength due to outdoor environment can also be attributed to the degraded epoxy properties since unlike the control specimens, very thin or almost no concrete layer was found to be attached to debonded FRP for exposed specimens.

The change in strain profiles, in terms of the loads at the shifting of initial stress transfer length, and increase in effective bond lengths were identified.

Based on the findings, it can be concluded that the outdoor environment caused the highest degradation of GFRP-concrete pull-out strength, whereas degradation of pull-out strength due to wet-dry cycles was slightly lower. The change of failure modes for these two conditions suggests the dependence of pull-out strength more on epoxy properties. However, further research needs to be conducted on the effect of similar conditions on epoxy properties to validate this. Increased effective bond lengths for all three conditions necessitates the design of bond length longer than the effective bond length of unexposed conditions for achieving the full capacity of bond strength in long term. Temperature cycles did not have any negative effect on bond strength and failure modes. However, further study with lowering the minimum temperature will increase the difference between the maximum and minimum temperature of the temperature envelope and may lead to different findings.

## Acknowledgments

The authors acknowledge the financial and technical support provided by Centre for Built Infrastructure Research (CBIR) at University of Technology Sydney (UTS) for conducting the experimental studies.

## Open Access

This article is distributed under the terms of the Creative Commons Attribution 4.0 International License (<http://creativecommons.org/licenses/by/4.0/>), which permits unrestricted use, distribution, and reproduction in any medium, provided you give appropriate credit to the original author(s) and the source, provide a link to the Creative Commons license, and indicate if changes were made.

## References

- Al-Tamimi, A. K., Hawileh, R. A., Abdalla, J. A., Rasheed, H. A., & Al-Mahaidi, R. (2014). Durability of the bond between CFRP plates and concrete exposed to harsh environments. *Journal of Materials in Civil Engineering*, 27, 04014252.
- AS 1012.17. (1997). *Method of testing concrete—Determination of the static chord modulus of elasticity and Poisson's ratio of concrete specimens*. Sydney, Australia: Standards Australia.
- AS 1012.9. (1999). *Method of testing concrete—Determination of the compressive strength of concrete specimens*. Sydney, Australia: Standards Australia.
- ASTM D3039/D3039M. (2008). *Standard test method for tensile properties of polymer matrix composite materials*. Pennsylvania: American Society for Testing and Materials (ASTM).
- Benzarti, K., Chataigner, S., Quiertant, M., Marty, C., & Aubagnac, C. (2011). Accelerated ageing behaviour of the adhesive bond between concrete specimens and CFRP overlays. *Construction and Building Materials*, 25, 523–538.
- Bizindavyi, L., & Neale, K. (1999). Transfer lengths and bond strengths for composites bonded to concrete. *Journal of Composites for Construction*, 3, 153–160.
- Chajes, M. J., Thomson, T. A., & Farschman, C. A. (1995). Durability of concrete beams externally reinforced with composite fabrics. *Construction and Building Materials*, 9, 141–148.
- Chen, J., & Teng, J. (2001). Anchorage strength models for FRP and steel plates bonded to concrete. *Journal of Structural Engineering*, 127, 784–791.
- Dai, J., Ueda, T., & Sato, Y. (2005). Development of the non-linear bond stress-slip model of fiber reinforced plastics

- sheet–concrete interfaces with a simple method. *Journal of Composites for Construction*, 9, 52–62.
- Dai, J. G., Yokota, H., Iwanami, M., & Kato, E. (2010). Experimental investigation of the influence of moisture on the bond behavior of FRP to concrete interfaces. *Journal of Composites for Construction*, 14, 834.
- Dejke, V., & Tepfers, R. (2001). Durability and service life prediction of GFRP for concrete reinforcement. In *Proceedings of 5th international conference on fiber-reinforced plastics for reinforced concrete structures (FRPRCS-5)* (pp. 505–516).
- Grace, N. F. (2004). Concrete repair with CFRP. *Concrete International*, 26, 45–52.
- Homam, S., Sheikh, S., & Mukherjee, P. (2001). Durability of fibre reinforced polymers (FRP) wraps and external FRP–concrete bond. In *Proceedings of the 3rd international conference on concrete under severe conditions*, Vancouver, BC, Canada, 18–20 June 2001, (pp. 1866–1873).
- Imani, F. S., Chen, A., Davalos, J. F., & Ray, I. (2010). Temperature and water-immersion effect on mode II fracture behavior of CFRP-concrete interface. In *CICE 2010—The 5th international conference on FRP composites in civil engineering*, Beijing, China (pp. 557–561).
- Kabir, M. I. (2014). Short and long term performance of concrete structures repaired/strengthened with FRP. PhD thesis, Civil Engineering, University of Technology, Sydney, Australia.
- Kabir, M. I., Samali, B., & Shrestha, R. (2016a). Fracture properties of CFRP–concrete bond subjected to three environmental conditions. *Journal of Composites for Construction*. doi:10.1061/(ASCE)CC.1943-5614.0000665
- Kabir, M. I., Shrestha, R., & Samali, B. (2016b). Effects of applied environmental conditions on the pull-out strengths of CFRP-concrete bond. *Construction and Building Materials*,. doi:10.1016/j.conbuildmat.2016.03.195.
- Kang, T. H.-K., Howell, J., Kim, S., & Lee, D. J. (2012). A state-of-the-art review on debonding failures of FRP laminates externally adhered to concrete. *International Journal of Concrete Structures and Materials*, 6, 123–134.
- Li, G., Pang, S., Helms, J., Mukai, D., Ibekwe, S., & Alaywan, W. (2002). Stiffness degradation of FRP strengthened RC beams subjected to hygrothermal and aging attacks. *Journal of Composite Materials*, 36, 795.
- Litherland, K. L., Oakley, D. R., & Proctor, B. A. (1981). The use of accelerated ageing procedures to predict the long term strength of GRC composites. *Cement and Concrete Research*, 11, 455–466.
- Lu, X. Z., Teng, J. G., Ye, L. P., & Jiang, J. J. (2005). Bond-slip models for FRP sheets/plates bonded to concrete. *Engineering Structures*, 27, 920–937.
- Mazzotti, C., Savoia, M., & Ferracuti, B. (2008). An experimental study on delamination of FRP plates bonded to concrete. *Construction and Building Materials*, 22, 1409–1421.
- Mazzotti, C., Savoia, M., & Ferracuti, B. (2009). A new single-shear set-up for stable debonding of FRP–concrete joints. *Construction and Building Materials*, 23, 1529–1537.
- Myers, J., Murthy, S., & Micelli, F. (2001). Effect of combined environmental cycles on the bond of FRP sheets to concrete. In *Proceedings of the international conference on composites in construction (CCC-2001)* Porto, Portugal, October 10–12, (pp. 55–59).
- Nishizaki, I., & Kato, Y. (2011). Durability of the adhesive bond between continuous fibre sheet reinforcements and concrete in an outdoor environment. *Construction and Building Materials*, 25, 515–522.
- Ouezdou, M. B., Belarbi, A., & Bae, S.-W. (2009). Effective bond length of FRP sheets externally bonded to concrete. *International Journal of Concrete Structures and Materials*, 3, 127–131.
- Phani, K. K., & Bose, N. R. (1987). Temperature dependence of hydrothermal ageing of CSM-laminate during water immersion. *Composites Science and Technology*, 29, 79–87.
- Robert, M., Wang, P., Cousin, P., & Benmokrane, B. (2010). Temperature as an accelerating factor for long-term durability testing of FRPs: Should there be any limitations? *Journal of Composites for Construction*, 14, 361.
- Shrestha, J., Ueda, T., & Zhang, D. (2014). Durability of FRP concrete bonds and its constituent properties under the influence of moisture conditions. *Journal of Materials in Civil Engineering*, 27, A4014009.
- Teng, J. G., Chen, J. F., Smith, S. T., & Lam, L. (2002). *FRP: Strengthened RC structures*. Hoboken, NJ: Wiley.
- Toutanji, H. A., & Gómez, W. (1997). Durability characteristics of concrete beams externally bonded with FRP composite sheets. *Cement & Concrete Composites*, 19, 351–358.
- Tuakta, C., & Büyüköztürk, O. (2011). Deterioration of FRP/concrete bond system under variable moisture conditions quantified by fracture mechanics. *Composites Part B Engineering*, 42, 145–154.
- Yuan, H., Teng, J. G., Seracino, R., Wu, Z. S., & Yao, J. (2004). Full-range behavior of FRP-to-concrete bonded joints. *Engineering Structures*, 26, 553–565.
- Yun, Y., & Wu, Y.-F. (2011). Durability of CFRP-concrete joints under freeze–thaw cycling. *Cold Regions Science and Technology*, 65, 401–412.